Title: Experimental verification of harvest induced instability in exploited populations

Authors: Luke A. Rogers*[,1], Zachary Moore[1], Abby Daigle[2], Pepijn Luijckx[3], and Martin Krkošek[1]

Affiliations
[1]Department of Ecology and Evolutionary Biology, University of Toronto, Toronto, ON
[2]Gulf Fisheries Centre, Fisheries and Oceans Canada, Moncton, NB
[3]School of Natural Sciences, Trinity College Dublin, Dublin, Ireland

*Corresponding author: luke.rogers@mail.utoronto.ca, +1-647-780-9304

Keywords
Empirical dynamic modeling, *Daphnia magna*, delay embedding, fishery, model-free forecasting, nonlinear deterministic process, oscillations, population dynamics, stability

Abstract

Harvesting has long been hypothesized to drive increased temporal variability in the abundance of exploited populations. However, distinct hypotheses are contentious. These include an erosion of equilibrium resilience (reduced recovery rate) that elevates the influence of environmental stochasticity versus an endogenous destabilization of deterministic nonlinear dynamics. The correct characterization is crucial for wildlife managers because the common assumption of equilibrium dynamics may obscure the risk of persistent collapse inherent in nonlinear tipping points and hysteresis. We conducted an experiment designed to distinguish the two mechanisms underlying harvest induced variability in exploited populations. Our experiment verified that harvest can amplify the variability in abundance of an exploited population. Our results indicated that variability in population abundance was governed by nonlinear deterministic dynamics including damped oscillations excited by chance perturbations, rather than stemming from environmental variability alone. This corroborated the growing body of evidence for the importance of deterministic nonlinear dynamics in exploited wildlife populations.

Introduction

Harvesting has long been hypothesized to drive increased temporal variability in the abundance of exploited populations. The original theory showed this effect in a logistic growth model of single population dynamics under harvest (Beddington and May 1977). The first empirical support came from long-term observations of larval abundance in exploited and unexploited fish species (Hsieh et al. 2006). Hypotheses to explain the underlying mechanism divide between effects driven by external forcing (EF) and by intrinsic dynamics (ID). The original theory showed that harvest led to increased return time (IRT-EF) to equilibrium following perturbations in abundance from external forcing (Beddington and May 1977). The variable fishing effect (VFE-EF) explained variability in exploited fish abundance by the direct effect of variability in fishing pressure on population dynamics (Jonzen et al. 2001, Jonzén et al. 2002).

The age truncation effect (ATE-EF) explained the increased variability by a reduction in capacity to buffer the population against external forcing represented by the loss of older, more fecund or more knowledgeable individuals (Berkeley et al. 2004, Anderson et al. 2008, Rouyer et al. 2012). A second age truncation effect (ATE-ID) explained the increased variability by a change in demographic parameters brought about by the loss of older individuals leading to increased expression of nonlinear deterministic intrinsic dynamics (Anderson et al. 2008, Munch et al. 2018).

The hypotheses that emphasize external forcing and internal dynamics have different management implications. The external forcing hypotheses (EF) correspond to equilibrium population dynamics with stochastic perturbations imposed by environmental variability (or fishing pressure in the case of VFE-EF). Equilibrium stochastic population dynamics are characterized by gradual change and low short term predictability. By contrast, the intrinsic dynamics hypothesis (ID) corresponds to nonlinear deterministic population dynamics in which abundance is governed by a deterministic process that fluctuates naturally or under excitation from perturbations. Nonlinear deterministic population dynamics are characterized by rapid change and high short term predictability.

The correct characterization of these dynamics is a challenge for wildlife managers who may be working with incomplete data. For example, current fisheries management assumes stable equilibrium stochastic dynamics from which reference points and maximum sustained yield (MSY) can be calculated (Hilborn and Walters 1992, Walters and Martell 2004). When the underlying dynamics are nonlinear deterministic, management assumptions may obscure the risk of reaching nonlinear thresholds or tipping points. Different from equilibrium stochastic dynamics that are generally resilient with reversible changes, nonlinear dynamics are inherently sensitive and may undergo catastrophic shifts that are difficult to reverse (Scheffer et al. 2001).

The relative importance of stochastic versus nonlinear deterministic processes in population dynamics touches at the heart of old questions of population regulation (Nicholson and Bailey 1935, Andrewartha and Birch 1954). Stochastic dynamics emphasize external forcing, while nonlinear deterministic dynamics focus on the intrinsic population dynamics (Grenfell et al. 1998, Bjornstad and Grenfell 2001, Scheffer et al. 2001, Stenseth et al. 2002). The extent to which nonlinear deterministic dynamics are present in natural populations is an active area of research (Hsieh et al. 2006, Munch et al. 2018). Environmental processes in the ocean have been characterized as predominantly linear stochastic, while the population dynamics of exploited fishes are increasingly recognized as nonlinear deterministic (Hsieh et al. 2006, Glaser et al. 2014, Munch et al. 2018). Hypothesized mechanisms to explain effect of harvest on variability in the abundance of exploited populations are divided between external forcing and internal dynamics. Consequently, they are divided between expectations that population dynamics of exploited species are linear stochastic versus nonlinear deterministic.

We conducted an experiment designed to distinguish the two mechanisms underlying harvest induced variability in exploited populations: stochasticity from external forcing and determinism from increased nonlinear instability. The experiment also verified that harvest

increased temporal variability in population size. We used unmanipulated populations in constant environments as a control, and added treatments for harvest and stochasticity in food supply in a factorial design, generating timeseries in abundance that lasted 50 census days. We used a combination of conventional statistics; model fitting, stability analysis and simulation of nonlinear mathematical models; and empirical dynamic modeling (EDM) to arrive at a mutually consistent explanation for the harvest effect from independent perspectives.

Methods

We used the widely studied *Daphnia magna* for our experiment (Ebert 2005). We maintained forty *Daphnia* populations in separate 4 L glass jars, each with 3.2 L standardized Artificial *Daphnia* Medium (ADaM) (Klüttgen et al. 1994). The populations were held at 21 °C in a climate-controlled chamber. All *Daphnia* came from the same clonal source (ref), and were constrained to reproduce by parthenogenesis. This ensured that genetic selection did not influence population demographic rates. The populations were exposed to 16 hr of light and 8 hr of darkness each day to mimic daylight in temperate latitudes. Populations were initially seeded with 150 individuals, and were allowed to stabilize for 130 days before the experiment began. Abundance and size-structure were estimated by census of a subsample at three-day intervals. The interval was chosen to approximate the time between successive clutches of clonal offspring for a typical adult female. Experimental treatments were applied and feeding took place at the same three-day interval, after subsampling. The experiment was maintained for 150 days, producing time-series of 50 points for adult and juvenile abundance in each population.

We used a randomized block design with four treatment levels: control, fished, stochastic, and fished & stochastic. There were ten replicate blocks in the experiment, with four populations each. Within each block the populations received different treatments. The interspersion of treatment levels within blocks was chosen to guard against nondemonic intrusion in the experiment (Hurlbert 1984). Populations were fed green algae (*Monoraphidium minutum*) at three-day intervals. The control and fished treatments received a constant quantity of green algae, while the stochastic and fished & stochastic treatments received a randomized quantity. The randomization was autocorrelated to mimic environmental stochasticity. The mean dose was equal so that all treatments received the same quantity of food over the length of the experiment. In the fished and fished & stochastic treatments, a constant fraction (40 %) of adult *Daphnia* were removed at the three-day interval. Size was used as a proxy for life stage. Adults were removed by filtration through a 1400 µm mesh screen. This mimicked fishing at a constant harvest effort for maximum sustained yield (MSY), a common management reference point (Hilborn and Walters 1992). The removal of adults but not juveniles corresponded to the size selectivity common in wild capture fisheries.

We used linear mixed effects models to estimate the treatment effects on *Daphnia* populations. We fit separate models to three response variables: the coefficients of variation (CV) in adult and juvenile abundances, and the percentage of the population made up by adults. The CVs and percent adults were calculated for each population. Adult CV represented the

temporal variability in the abundance of *Daphnia* that had recruited to the fishery or reproductive population. The percentage of adults represented the population stage-structure. We fit the models by maximum likelihood using the lme4 package (Bates et al. 2017) in R (R Core Team 2018). Treatment level was fit as a fixed effect, while experimental block was a random effect. We compared model fits with and without a random effect by AIC (Burnham and Anderson 2002).

We estimated *Daphnia* demographic parameters with two population models. In order to assess whether *Daphnia* populations could fluctuate under unstructured single-species dynamics alone, we first estimated the intrinsic rate of population growth from a model with strongly nonlinear (overcompensatory) density dependent mortality. The Ricker model was both strongly nonlinear and was shown to provide a robust measure of the intrinsic rate of population growth for iteroparous species (Myers et al. 1999). We linearized the Ricker model by a simple transformation, and fit the model by maximum likelihood using linear regression. The model was given by

$$\log_e\left(\frac{N_{i,j,t}}{e^{-F}N_{i,j,t-4}}\right) = a_j - b_j e^{-F} N_{i,j,t-4} + \varepsilon_{i,j,t} \quad (1)$$

where $N_{i,j,t}$ was adult abundance in replicate *i*, of treatment level *j*, at census *t*; e^{-F} = 1 or 0.6 was the per-census escapement from fishing; *a* was the intrinsic rate of population growth; *b* was a density dependent mortality parameter; and ε was the normally distributed residual error. We included a lag of four timesteps (twelve days) between reproduction and recruitment to account for the time to develop to maturity. We compared the model fit with and without a random effect for experimental block by AIC.

To make the *Daphnia* population dynamics comparable to a range of exploited fish stocks, we fit and analysed a structured single-species model. This second model accounted for the iteroparous life history by including a term for adults that survived from the previous census. The model was used by Shelton and Mangel (2011a) to characterize the stability of the structured single-species population dynamics of exploited fish stocks. The model was given by

$$N_{i,j,t} = e^{(-M_j - F)} N_{i,j,t-1} + N_{i,j,t-4}\alpha e^{(-F-\beta_j e^{-F} N_{i,j,t-4})} + \varepsilon_{i,j,t} \quad (2)$$

where *M* was the constant adult mortality rate, α was the maximum reproductive rate, β was a density dependent mortality parameter, and the remaining symbols were as defined for equation (1). We fit the model using the nlme package (Pinheiro et al. 2018) in R (R Core Team 2018). To assess the stability of the model, we derived an expression for the non-zero equilibrium in the absence of fishing, given by

$$N^* = \frac{-1}{\beta}\log_e\left(\frac{1 - e^{(-M)}}{\alpha}\right). \quad (3)$$

The equilibrium was positive (*i.e.* realistic) for $\alpha > (1 - e^{(-M)})$. We calculated the stability of the equilibria for the four treatment levels from the parameter estimates. Stability was characterized by the leading eigenvalue of the characteristic polynomial of the Jacobean matrix for equation (2). We estimated a 95% confidence interval around the absolute value of the leading eigenvalue, λ, by drawing 10,000 parameter combinations from a multivariate normal distribution with vector mean and variance-covariance matrix from the fitted model. We

calculated the characteristic return time to the non-zero equilibrium by $T_R = 1/(1 - |\lambda|)$ following Beddington *et al*. (1976) (Table A5). To compare model dynamics to *Daphnia* adult population dynamics we simulated adult abundance data from equation (2). We used parameter estimate mean values for the deterministic part of the simulation model. We used a normally distributed error term equal to one-third of the residual error from the fitted model for each treatment for the stochastic part of the simulation. This reduced residual error ensured that no populations went extinct. We simulated fifty observations after a discarded burn-in for ten replicates of each of the four treatments.

We used empirical dynamic modeling to compare the deterministic skeletons of the *Daphnia* population dynamics among the four treatment levels. Empirical dynamic modeling (EDM) is a type of model-free forecasting in which delay-embeddings of a time series can be used to reconstruct key features of an underlying dynamical process (Ye et al. 2015). The key features we were interested in were the embedding dimension and the degree of nonlinearity that best characterised the population dynamics in the replicates of each treatment. These two parameters are commonly estimated in sequence: the embedding dimension first by the method of simplex projection (Sugihara and May 1990), and the degree of nonlinearity second, and conditional on the embedding dimension, by *S*-mapping (Sugihara 1994). Because both methods are more robust for longer time series (100s rather than 10s of observations) we used the method of dewdrop regression to concatenate the time series from replicates within each treatment (Hsieh et al. 2008). The resulting composite time series satisfied the assumption that component time series must derive from the same dynamical process because each replicate time series came from the same experimental treatment in controlled laboratory conditions.

We then used simplex projection and *S*-mapping to characterise the composite time-series dynamics. We first-differenced each of the four composite time series to remove the effects of lag-1 autocorrelation and then standardised the them to zero mean and unit standard deviation (Sugihara and May 1990). We estimated the optimal embedding dimension and nonlinearity parameter for each treatment in the ranges 1–10 and 0–8 respectively. The optimal embedding dimension (E) is commonly connected to the number of state variables (D) in the underlying process by the inequality $E < 2D + 1$ (Takens 1981, Sugihara and May 1990). The nonlinearity parameter (θ) weights local values (in space rather than time) more heavily as it increases, yielding a simple autoregressive process at zero and more locally weighted maps as θ increases (Sugihara 1994). We tested the significance of θ for each treatment by bootstrapping *p*-values from surrogate data. To generate the surrogate data, we randomized the phases of the Fourier transform of each component time series within each composite, while preserving the power spectrum of the component. We used the rEDM package (Ye et al. 2017) for simplex projection, *S*-mapping and bootstrapping *p*-values.

Results

The *Daphnia* fishery experiment produced ten time series of population abundance for each of four treatments: control, fished, stochastic, and fished & stochastic (Figures 1). The time series were 50 observations in length, except for the four treatments in block D which were cut short

by ten observations to remove a feeding error after census 40 (Figure B1). Adult CV was significantly higher in the fished treatment relative to the control, and higher but not significantly so in the fished & stochastic treatment relative to the stochastic treatment (Figure 2, Table A1). This result gave strong evidence that fishing increased the temporal variability in abundance of *Daphnia* populations. By contrast, juvenile CV was significantly higher in the two stochastic treatments, relative to the fished and control treatments. The percentage of adults was highest in the control treatment, lower in the stochastic treatment, and lowest in the two fished treatments (Figure 3). Mean adult abundance was lower in the two fished treatments than in the control and stochastic treatments. Mean juvenile abundance was higher in the two stochastic treatments than in the control and fished treatments. The intrinsic rate of population growth estimated from equation (1) was higher in the two fished treatments than in the control and stochastic treatments (Table A2).

The second model confirmed the results of the first and gave a more nuanced picture of the *Daphnia* population dynamics. Both the intrinsic rate of population growth and the maximum reproductive rate were higher in the two fished treatments than in the control and stochastic treatments (Table A3, A4). The intrinsic rate of population growth was estimated by the absolute value of the dominant eigenvalue for the Jacobean matrix at the extinction equilibrium. The maximum reproductive rate was estimated by the α parameter in equation (2). While adult natural mortality was not significantly different among the four treatments, the range of uncertainty was several times higher for the fished treatment than the other three treatments (Figure 4, Table A3). Model dynamics grew monotonically away from the extinction equilibrium for all four treatments (Table A4).

The combination of the natural mortality rate and the maximum reproductive rate determined the model stability around the non-zero equilibrium. The characteristic return time following perturbation was significantly higher for the two fished treatments than for the control and stochastic treatments (Table A5). For the two fished treatments the model was stable with damped oscillations (Figure 4, Table A4). For the control and stochastic treatments the parameter means corresponded to stable damped oscillations while the 95 % confidence intervals overlapped the boundary between monotone stability and damped oscillations (Figure 4). The simulations from equation (2) showed a higher CV for the two fished treatments relative to the control and stochastic treatments (Figure 5). This was consistent with the adult CV by treatment from the *Daphnia* experiment.

Empirical dynamic modeling characterised the *Daphnia* population dynamics independent of the model-fitting analysis. The optimal embedding dimensions were three for the control and fished treatments, four for the stochastic treatment, and five for the fished & stochastic treatment (Table 1). These indicate that the underlying process dimensions may be in the range of 2–3 for the control and fished treatments, 2–4 for the stochastic treatment, and 3–5 for the fished & stochastic treatment (Sugihara and May 1990). The nonlinearity parameters for all four treatments were significantly greater than zero. This provided evidence that a low-dimensional deterministic nonlinear process was an important part of the *Daphnia* population dynamics for all four treatments. The nonlinearity parameter for the fished treatment was

higher than for the other three treatments. Similarly, the forecast accuracy which is the Pearson correlation coefficient between predicted and observed values was higher for the fished treatment than for the other three treatments.

Discussion

Our results provide experimental verification that a constant harvest rate can increase temporal variability in the abundance of exploited populations. The coefficient of variation was higher in harvested treatments relative to controls. This result was first proposed by Beddington and May (1977), who showed theoretically that for a population with logistic growth, the return time to equilibrium following perturbation is slower due to harvest. Empirical confirmation from marine fish was for long hampered by the scarcity of data for paired harvested and unharvested populations of the same species in comparable environments. Hsieh *et al*. (2006) reported higher variability in fished populations by comparing larval abundances of fished and unfished species in coastal waters while accounting for differences in life history traits. Our results confirm that harvesting increases temporal variation in population size, using clonally reproducing populations of the same line in a controlled laboratory environment.

Our results help discriminate among proposed mechanisms that link harvest to increased variability in population abundance. These mechanisms include the variable fishing effect (VFE-EF), increased return time (IRT-EF), and age truncation effect (ATE-EF) associated with external forcing, and the age truncation effect (ATE-ID) due to intrinsic dynamics (Beddington and May 1977, Jonzen et al. 2001, Anderson et al. 2008). Because we used a constant harvest rate, our results showed that the VFE-EF mechanism was not necessary for harvest to increase variability in population abundance. Our results did show slower characteristic return time to equilibrium in the fished treatments, initially consistent with the IRT-EF mechanism (Table A5). Harvest also reduced the proportion of adults in fished treatments, consistent with an age truncation effect (Figure 3), which may reduce the capacity of a population to buffer against environmental variability (Berkeley et al. 2004, Shelton and Mangel 2011a). However, variability in adult abundance was not significantly higher in the fished & stochastic treatment relative to the fished treatment, indicating that the IRT-EF and ATE-EF mechanisms did not play an important role. External forcing represented by environmental variability in the stochastic treatments did not explain the effect of harvest on the variability in adult *Daphnia* abundance.

Changes to the intrinsic dynamics from altered demographic parameters explained the harvest effect on *Daphnia* population variability. The two fished treatments had higher intrinsic population growth rates than the control and stochastic treatments (Tables A2 and A4). Increased growth rates have been associated with more strongly nonlinear—more state-dependent—dynamics in some simple population models (May 1976). This analogy is appropriate because the population dynamics of all treatments were nonlinear, with the fished treatment more nonlinear than the control (Table 1). Nonlinear dynamics include damped oscillations in which population abundance overshoots equilibrium following perturbation, persistent limit cycles, and chaos (Kot 2001). The population dynamics from the parameterized

equation (2) were in the stable damped oscillation region of the stability landscape for all four treatments. This was consistent with the finding that among 45 exploited fish species demographic parameter estimates predicted only three would exhibit persistent limit cycles or chaos (Shelton and Mangel 2011a). The two fished treatments were closer to the unstable region of the stability landscape, while the 95 % confidence intervals for the control and stochastic treatments overlapped the monotonic stable region (Figure 4). This was consistent with the interpretation that the population dynamics of the two fished treatments were more sensitive to perturbation than the control and stochastic treatments. Variability in population abundance may have resulted from the convolution of chance perturbations in abundance with nonlinear intrinsic dynamics that varied in their sensitivity due to changes in the population growth rates brought on by harvest (Anderson et al. 2008, Shelton and Mangel 2011b, Sugihara et al. 2011). This interpretation was consistent with the ATE-ID mechanism, although we emphasize that changes to the age structure may have been incidental. If a low threshold of perturbations was sufficient to excite the nonlinear dynamics in the fished treatment, the environmental variability may have worked to overwhelm rather than amplify the nonlinear dynamics in the two stochastic treatments.

Our results confirm that harvest can induce population dynamics that are different from those predicted by conventional management models. Conventional management models typically assume a stable equilibrium, for example at MSY, and stochastic fluctuations around that equilibrium that stem from environmental variability (Hilborn and Walters 1992, Walters and Martell 2004). Our results indicate that variability in population abundance was governed by nonlinear deterministic dynamics including damped oscillations excited by chance perturbations, rather than stemming from environmental variability alone. Our results are consistent with the findings of Hsieh *et al*. (2005) and Munch *et al*. (2018) who show that a substantial portion of the variability in marine fish population dynamics derived from nonlinear deterministic rather than equilibrium stochastic processes. Our findings add further support to the seemingly paradoxical conclusion that exploited population can exhibit both more variable and simultaneously more predictable population dynamics.

Our finding that harvest can increase the temporal variability in population abundance via amplified nonlinear dynamics has significant implications for wildlife management and conservation. Equilibrium stochastic dynamics typically respond proportionally to external forcing and change gradually over time. By contrast, nonlinear deterministic dynamics are characterized by sensitivity to ecosystem conditions and may undergo sudden persistent change. For example, nonlinear amplification produces dynamical responses disproportional to inputs (Dixon et al. 1999), while critical transitions can move population dynamics between alternative stable states that may be difficult to reverse due to hysteresis (Scheffer et al. 2001). Effective management depends on accurately forecasting the consequences of prospective management decisions. Forecast abilities for stochastic versus nonlinear dynamics are inherently different. Nonlinear dynamics yield more accurate short term forecasts than stochastic dynamics, because deterministic processes are predictable over short forecast horizons (Sugihara 1994, Glaser et al. 2014). By contrast, nonlinear dynamics yield less accurate

long term forecasts than stochastic dynamics, because nonlinear processes propagate and are sensitive to small perturbations in abundance (Sugihara 1994).

Increased variability in population abundance can also lead to undesirable consequences. In a feedback between coupled human and natural systems, increased population variability due to harvest may increase variability in harvest quotas including more frequent resource closures (Liu et al. 2007). Variable quotas and more frequent closures can lead to economic hardship for communities that rely on natural resources. Ecological affects may also occur including changes to population persistence. Harvest typically decreases mean population abundance except in extreme cases (Abrams 2009). The combination of decreased mean abundance and increased variability indicates that exploited populations may experience increased risk of collapse by this combined effect of harvest. How the risk of collapse is realized in nature and whether local collapse may be reversed depends on features of population spatial structure and synchrony among other factors (Hanski 1998, Fox et al. 2017).

Our conclusions were strengthened by drawing on independent lines of evidence. The iteroparous model in equation (2) was valuable for its simplicity, tractability, and comparability to the analysis made by Shelton and Mangel (2011a). The simplicity made model fitting possible within a maximum likelihood framework, and allowed a straightforward stability analysis to characterize the equilibrium stability. Simulations from the fitted model recapitulated the patterns in CV across treatments from the *Daphnia* experiment, indicating that the model captured the relevant dynamics. The empirical dynamic modeling (EDM) provided independent confirmation that a significant portion of the dynamics of all four treatments were governed by a nonlinear deterministic process (Table 1). This result justified our choice of strongly nonlinear density dependent mortality in equation (2). The higher forecast accuracy and stronger nonlinearity in the fished treatment compared to the control treatment support the interpretation from the parameter estimation and stability analysis that an increased growth rate pushed the population dynamics of the fished treatment into a region of greater nonlinearity than the control treatment.

The EDM approach was well-suited for the analysis of our abundance time series data. Because EDM relies on a delay-embedding of time series observations, no prior assumptions about functional form were made (Sugihara and May 1990, Sugihara et al. 1990, Sugihara 1994). This flexibility adds credence to the characterization of the deterministic component of time series dynamics. Strongly nonlinear population dynamics in *Daphnia* are not surprising because similar dynamics have been shown to underlie a growing number of ecological systems (Sugihara and May 1990, Hsieh et al. 2005, Sugihara et al. 2012, Ye et al. 2015, Munch et al. 2018). EDM assumes that the time series under analysis were generated by a stationary process (Sugihara 1994). While this criterion may be difficult to verify for wild systems, our time series data derived from a controlled experiment in which all populations were exposed to stable average conditions.

The experimental design includes several caveats. Experimental *Daphnia* populations differed from exploited wildlife populations in a number of respects. *Daphnia* lines were clonal

to remove evolutionary effects, but this may also have removed natural population diversity. Population diversity comes in many types (e.g. genetic, spatial), but is generally thought to stabilize population dynamics in the wild (Schindler et al. 2010). *Daphnia* food webs consisting of a single resource were far simpler than food webs in the wild. These populations were resource limited, possibly similar to exploited top predators but different from species that experience heavy predation such as forage fish. *Daphnia* reproduced continuously different from the pulsed annual reproduction common to many exploited fishes. While the overall effect of harvest on experimental *Daphnia* population dynamics was the same as predicted and observed for exploited populations in the wild (Beddington and May 1977, Hsieh et al. 2006), the differences between the experimental and natural systems should not be understated. The mechanisms underlying harvest induced increase in the variability of population abundance may be several and quite different between the two settings. Nevertheless, the use of real biological populations in replicated treatments strengthens the connection between theory and exploited population in the wild. The concurrence between the effect of harvest on variability in population abundance in theory, experimentation, and observational studies suggests that the effect may be general.

The source of the perturbations suggested to excite the otherwise stable nonlinear dynamics required consideration. The overt stochastic forcing in the experiment derived from a randomized feeding regime, but this was restricted to the two stochastic treatments. Because nonlinear deterministic dynamics were detected in all four treatments, but the dynamics were characterized stable damped oscillations, there may have been some different source of perturbations in adult abundance. Interaction between adult and juvenile stage classes was a likely candidate. For example, competition between two stage classes vying for a common resource was shown to induce population cycles in theoretical models (de Roos and Persson 2003). Alternatively, food dependent individual growth was shown to create overcompensatory population dynamics within stage classes also in theoretical models (De Roos et al. 2007). Either of these mechanisms could in principle have created perturbations in adult abundance independent of environmental stochasticity sufficient to excite the observed nonlinear dynamics.

In conclusion, our study verified that harvest can amplify the variability in abundance of an exploited population. This result is significant for the persistence of exploited wildlife populations, and the economic stability of communities that harvest wildlife. The stochastic or deterministic nature of the population dynamics of exploited species has crucial implications for the ability to forecast the effects of management decisions or reverse ecosystem shifts. Our results provide an important link between ecological theory and observational studies to verify the harvest effect.

Acknowledgements

This work was supported by an NSERC Alexander Graham Bell Canada Graduate Scholarship to L.A.R., NSERC USRA awards to Z.M. and A.D., and an NSERC Discovery Grant and Canada Research Chair to M.K.

References

Abrams, P. A. 2009. When does greater mortality increase population size? the long history and diverse mechanisms underlying the hydra effect. Ecology Letters 12:462–474.

Anderson, C. N. K., C. Hsieh, S. A. Sandin, R. Hewitt, A. Hollowed, J. Beddington, R. M. May, and G. Sugihara. 2008. Why fishing magnifies fluctuations in fish abundance. Nature 452:835–839.

Andrewartha, H. G., and L. C. Birch. 1954. The Distribution and Abundance of Animals. University of Chicago Press, Chicago, IL.

Bates, D., B. Bolker, S. Walker, H. Singmann, B. Dai, F. Scheipl, G. Grothendiech, and P. Green. 2017. Package 'lme4.'

Beddington, J. R., C. A. Free, and J. H. Lawton. 1976. Concepts of Stability and Resilience in Predator-Prey Models. Journal of Animal Ecology 45:791–816.

Beddington, J. R., and R. M. May. 1977. Harvesting Natural Populations in a Randomly Fluctuating Environment. Science 197:463 LP-465.

Berkeley, S. A., M. a Hixon, R. J. Larson, and M. S. Love. 2004. Fisheries Sustainability via protection of age structure and spatial distribution of fish populations. Am. Fisheries Soc. 29:23–32.

Bjornstad, O. N., and B. T. Grenfell. 2001. Noisy Clockwork: Time Series Analysis of Population Fluctuations in Animals. Science 293:638–643.

Burnham, K. P., and D. R. Anderson. 2002. Model Selection and Multimodel Inference: A Practical Information-Theoretic Approach (2nd ed). Page Ecological Modelling.

Dixon, P. A., M. J. Milicich, and G. Sugihara. 1999. Episodic Fluctuations in Larval Supply. Science 283:1528–1530.

Ebert, D. 2005. Ecology, epidemiology and evolution of parasitism in *Daphnia*. National Library of Medicine (US), National Centre for Biotechnology Information., Bethesda, MD.

Fox, J. W., D. Vasseur, M. Cotroneo, L. Guan, and F. Simon. 2017. Population extinctions can increase metapopulation persistence. Nature Ecology & Evolution 1:1271–1278.

Glaser, S. M., M. J. Fogarty, H. Liu, I. Altman, C. Hsieh, L. Kaufman, A. D. MacCall, A. A. Rosenberg, H. Ye, and G. Sugihara. 2014. Complex dynamics may limit prediction in marine fisheries. Fish and Fisheries 15:616–633.

Grenfell, B. T., K. Wilson, B. F. Finkenstadt, T. N. Coulson, S. Murray, S. D. Albon, J. M. Pemberton, T. H. Clutton-Brock, and M. J. Crawley. 1998. Noise and determinism in synchronized sheep dynamics. Nature 394:674–677.

Hanski, I. 1998. Metapopulation dynamics. Nature 396:41–49.

Hilborn, R., and C. J. Walters. 1992. Quantitative fisheries stock assessment: choice, dynamics and uncertainty. Routledge, Chapman & Hall.

Hsieh, C., C. Anderson, and G. Sugihara. 2008. Extending nonlinear analysis to short ecological time series. Amer. Natur. 171:71–80.

Hsieh, C., S. M. Glaser, A. J. Lucas, and G. Sugihara. 2005. Distinguishing random environmental fluctuations from ecological catastrophes for the North Pacific Ocean. Nature 435:336–340.

Hsieh, C., C. S. Reiss, J. R. Hunter, J. R. Beddington, R. M. May, and G. Sugihara. 2006. Fishing elevates variability in the abundance of exploited species. Nature 443:859–862.

Hurlbert, S. H. 1984. Pseudoreplication and the Design of Ecological Field Experiments.

481 Ecological Monographs 54:187–211.
482 Jonzen, N., P. Lundberg, M. Cardinale, and F. Arrhenius. 2001. Variable fishing mortality and the
483 possible commercial extinction of the eastern Baltic cod. Marine Ecology Progress Series
484 210:291–296.
485 Jonzén, N., J. Ripa, and P. Lundberg. 2002. A Theory of Stochastic Harvesting in Stochastic
486 Environments. The American Naturalist 159:427–437.
487 Klüttgen, B., U. Dülmer, M. Engels, and H. T. Ratte. 1994. ADaM, an artificial freshwater for the
488 culture of zooplankton. Water Research 28:743–746.
489 Kot, M. 2001. Elements of mathematical ecology. Cambridge University Press, Cambridge.
490 Liu, J., T. Dietz, S. R. Carpenter, M. Alberti, C. Folke, E. Moran, A. N. Pell, P. Deadman, T. Kratz, J.
491 Lubchenco, E. Ostrom, Z. Ouyang, W. Provencher, C. L. Redman, S. H. Schneider, and W. W.
492 Taylor. 2007. Complexity of Coupled Human and Natural Systems. Science 317:1513–1516.
493 May, R. 1976. Simple mathematical models with very complicated dynamics. Nature 261:459–
494 67.
495 Munch, S. B., A. Giron-Nava, and G. Sugihara. 2018. Nonlinear dynamics and noise in fisheries
496 recruitment: A global meta-analysis. Fish and Fisheries 0.
497 Myers, R. A., K. G. Bowen, and N. J. Barrowman. 1999. Maximum reproductive rate of fish at
498 low population sizes. Canadian Journal of Fisheries and Aquatic Sciences 56:2404–2419.
499 Nicholson, A. J., and V. A. Bailey. 1935. The Balance of Animal Populations. Part I. Proceedings
500 of the Zoological Society of London 105:551–598.
501 Pinheiro, J., D. Bates, S. DebRoy, D. Sarkar, and R Core Team. 2018. {nlme}: Linear and
502 Nonlinear Mixed Effects Models.
503 R Core Team. 2018. R: A Language and Environment for Statistical Computing. Vienna, Austria.
504 de Roos, A. M., and L. Persson. 2003. Competition in size-structured populations: mechanisms
505 inducing cohort formation and population cycles. Theoretical Population Biology 63:1–16.
506 De Roos, A. M., T. Schellekens, T. van Kooten, K. van de Wolfshaar, D. Claessen, and L. Persson.
507 2007. Food-Dependent Growth Leads to Overcompensation in Stage-Specific Biomass
508 When Mortality Increases: The Influence of Maturation versus Reproduction Regulation.
509 The American Naturalist 170:E59–E76.
510 Rouyer, T., A. Sadykov, J. Ohlberger, and N. C. Stenseth. 2012. Does increasing mortality change
511 the response of fish populations to environmental fluctuations? Ecology Letters 15:658–
512 665.
513 Scheffer, M., S. Carpenter, J. A. Foley, C. Folke, and B. Walker. 2001. Catastrophic shifts in
514 ecosystems. Nature 413:591–596.
515 Schindler, D., R. Hilborn, B. Chasco, C. Boatright, T. Quinn, L. Rogers, and M. Webster. 2010.
516 Population diversity and the portfolio effect in an exploited species. Nature 465:609–13.
517 Shelton, A. O., and M. Mangel. 2011a. Fluctuations of fish populations and the magnifying
518 effects of fishing. Proceedings of the National Academy of Sciences 108:7075–7080.
519 Shelton, A. O., and M. Mangel. 2011b. Reply to Sugihara et al: The biology of variability in fish
520 populations. Proceedings of the National Academy of Sciences 108:E1226–E1226.
521 Stenseth, N. C., A. Mysterud, G. Ottersen, J. Hurrell, K. Chan, and M. Lima. 2002. Ecological
522 effects of climate fluctuations. Science 297:1292–6.
523 Sugihara, G. 1994. Nonlinear forecasting for the classification of natural time series. Phil. Trans.
524 Roy. Soc. Lond. A 348:477–95.

Sugihara, G., J. Beddington, C. Hsieh, E. Deyle, M. Fogarty, S. M. Glaser, R. Hewitt, A. Hollowed, R. M. May, S. B. Munch, C. Perretti, A. A. Rosenberg, S. Sandin, and H. Ye. 2011. Are exploited fish populations stable? Proceedings of the National Academy of Sciences 108:E1224–E1225.

Sugihara, G., B. Grenfell, and R. May. 1990. Distinguishing error from chaos in ecological time series. Phil. Trans. Roy. Soc. Lond. B 330:235–51.

Sugihara, G., and R. May. 1990. Nonlinear forecasting as a way of distinguishing chaos from measurement error in time series. Nature 344:734–41.

Sugihara, G., R. May, H. Ye, C. Hsieh, E. Deyle, M. Fogarty, and S. Munch. 2012. Detecting causality in complex ecosystems. Science 388:496–500.

Takens, F. 1981. Detecting strange attractors in turbulence. Pages 366–381 *in* D. Rand and L. Young, editors. Dynamical systems and turbulence, Warwick 1980. Springer, Berlin.

Walters, C. J., and S. J. D. Martell. 2004. Fisheries ecology and management. Princeton University Press, Princeton, NJ.

Ye, H., R. Beamish, S. Glaser, S. Grant, C. Hsieh, L. Richards, J. Schnute, and G. Sugihara. 2015. Equation-free mechanistic ecosystem forecasting using empirical dynamic modeling. Proc. Natl. Acad. Sci.:E1569-76.

Ye, H., A. Clark, E. Deyle, S. Munch, O. Keyes, J. Cai, E. White, J. Cowles, J. Stagge, Y. Daon, A. Edwards, and G. Sugihara. 2017. rEDM: Applications of Empirical Dynamic Modeling from Time Series.

Figures

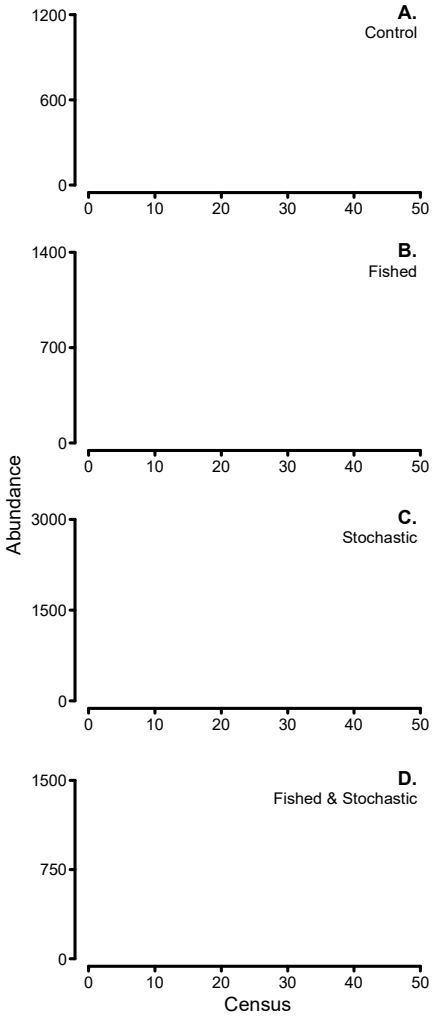

Figure 1. Median *Daphnia* abundance (line) with 2.5–97.5 % quantile range (shaded). Juvenile (light grey) and adult abundance (dark grey) shown. Treatments are: **A.** Control, **B.** Fished, **C.** Stochastic, and **D.** Fished & stochastic.

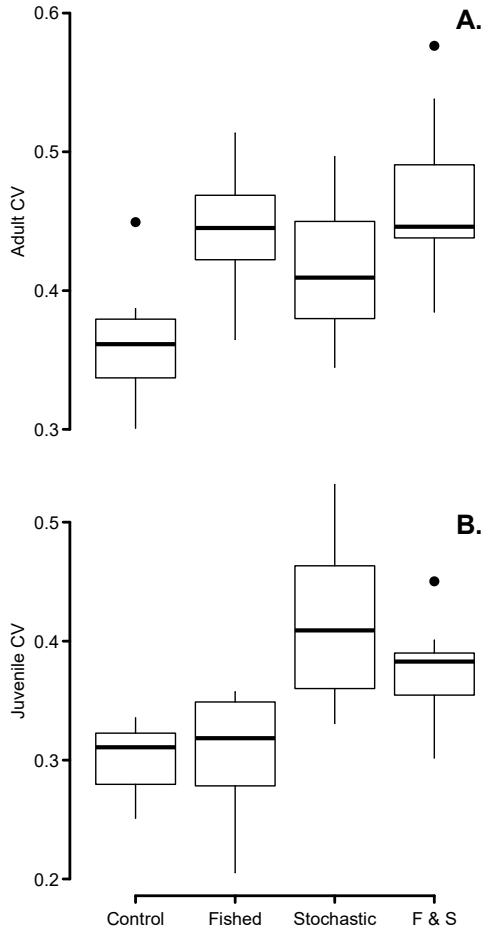

Figure 2. Boxplots showing coefficient of variation for all ten replicates within each treatment. Shown are: **A.** adult CV, **B.** juvenile CV.

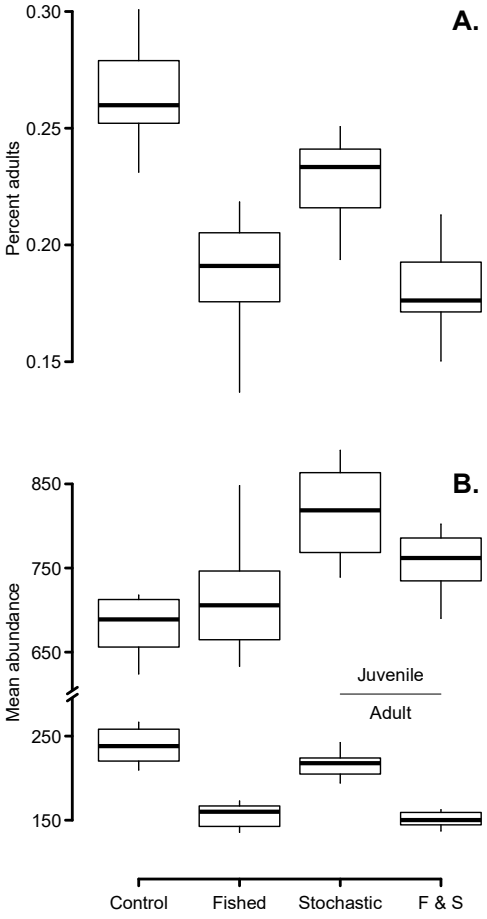

Figure 3. Boxplots showing **A.** the percent adults and **B.** the mean abundance of juvenile and adult *Daphnia* for all ten replicates within each treatment.

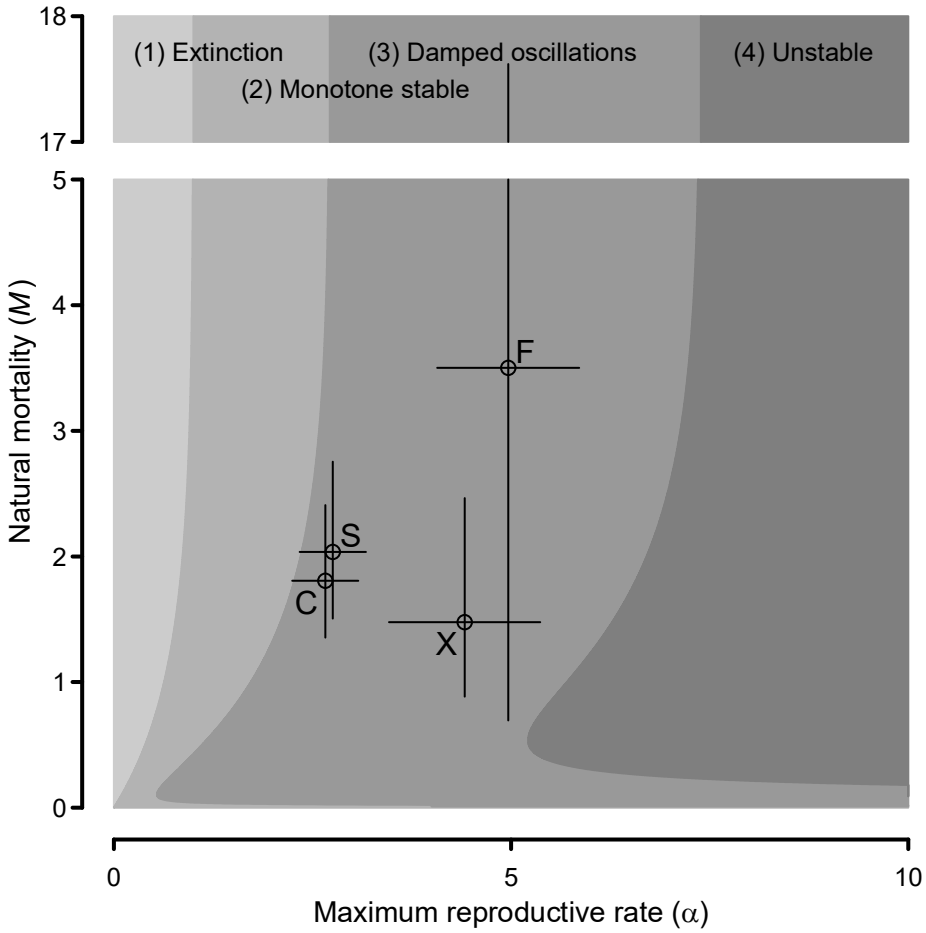

Figure 4. Stability surface of the iteroparous model with parameter estimates (open circles) and 95 % confidence intervals (lines) for each of the four treatments. Stability regions for the model are: Extinction (light grey), monotonic stability (light mid-grey), damped oscillations (dark mid-grey), and unstable (dark grey). Shown are natural mortality (*y*-axis) and maximum reproductive rate (*x*-axis) estimates for: control (C), fished (F), stochastic (S) and fished & stochastic (X) treatments.

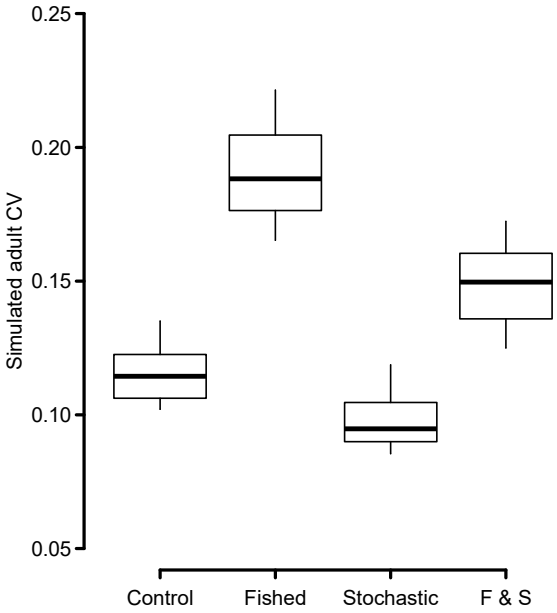

Figure 5. Boxplots showing coefficient of variation for adult abundance simulated from equation (2). Ten replicates of fifty observations for each treatment were generated. Simulation parameters were mean estimates from the fitted model. Normally distributed process error was one-third of the fitted residual error for each treatment to prevent extinction.

Tables

Table 1. Empirical dynamic modeling of *Daphnia* population dynamics. Parameters including embedding dimension *E*, nonlinearity parameter θ, and forecast accuracy reported as Pearson correlation coefficient between predicted and observed values ρ. The increase in forecast accuracy relative to the linear autoregressive model ($\theta = 0$) is given by $\Delta\rho$.

Treatment	***E***	θ	ρ	$\Delta\rho$	***p***
Control	3	1.00	0.553	0.0085	0.0299
Fished	3	4.00	0.639	0.0336	0.0050
Stochastic	4	1.50	0.576	0.0083	0.0249
Fished & Stochastic	5	1.50	0.586	0.0193	0.0100

Appendix A: Tables

Table A1. Linear mixed effects model fits for adult CV, juvenile CV, and percent adults. Fixed effects were the four treatment levels. The random effect was the experimental block. Shown are the fixed effect coefficient estimates and 95 % confidence intervals (mean $\pm$ 2 SE).

Response	Treatment	Estimate	95 % CI
Adult CV	Control	0.362	(0.331, 0.392)
	Fished	0.444	(0.414, 0.475)
	Stochastic	0.414	(0.383, 0.445)
	Fished & Stochastic	0.464	(0.433, 0.494)
Juvenile CV	Control	0.299	(0.263, 0.336)
	Fished	0.307	(0.271, 0.343)
	Stochastic	0.430	(0.394, 0.467)
	Fished & Stochastic	0.377	(0.340, 0.413)
Percent Adults	Control	0.265	(0.253, 0.278)
	Fished	0.187	(0.174, 0.199)
	Stochastic	0.227	(0.215, 0.240)
	Fished & Stochastic	0.182	(0.169, 0.194)

582

Table A2. Fit of the Ricker model to *Daphnia* adult population growth. The model was fitted by maximum likelihood as a simple linear regression with independent intercept and slope for each experimental treatment. The expression of the model is given by equation (1).

Coefficient	***a***	**95% CI$_a$**	***b***	**95% CI$_b$**
Control	1.084	(0.926, 1.242)	0.0046	(0.0040, 0.0052)
Fished	1.700	(1.566, 1.834)	0.0130	(0.0117, 0.0143)
Stochastic	1.064	(0.993, 1.135)	0.0049	(0.0043, 0.0055)
Fished & Stochastic	1.685	(1.619, 1.751)	0.0129	(0.0116, 0.0142)

583

584

Table A3. Fit of the iteroparous model given by equation (2). The model was fitted by maximum likelihood. Parameter estimates and 95 % confidence intervals are shown.

Coefficient	Parameter	Group	Estimate	95% CI
Adult mortality	M	Control	1.806	(1.35, 2.41)
		Fished	3.501	(0.70, 17.62)
		Stochastic	2.036	(1.51, 2.75)
		Fished & Stochastic	1.477	(0.89, 2.47)
Maximum reproductive rate	α	Control	2.661	(2.25, 3.08)
		Fished	4.964	(4.07, 5.86)
		Stochastic	2.756	(2.34, 3.17)
		Fished & Stochastic	4.416	(3.46, 5.37)
Density dependent mortality	β	Control	0.005	(0.004, 0.005)
		Fished	0.011	(0.010, 0.013)
		Stochastic	0.005	(0.004, 0.006)
		Fished & Stochastic	0.011	(0.010, 0.013)

585
586

587
588

Table A4. Local stability of the zero and non-zero equilibrium for the iteroparous model in equation (2). Stability is calculated with $F = 0$ to emphasize the intrinsic dynamics. Confidence intervals were bootstrapped using 10,000 random draws from a multivariate normal parameter distribution with means and variance-covariance matrix from the fitted model.

Treatment	N^*	λ_{N^*}	$\lvert\lambda_{N^*}\rvert$	95% CI$_{\lvert\lambda\rvert}$	Stability	Behaviour
Control	0	$1.32 + 0i$	1.32	(1.280, 1.360)	Unstable	Monotone
Fished	0	$1.50 + 0i$	1.50	(1.452, 1.603)	Unstable	Monotone
Stochastic	0	$1.32 + 0i$	1.32	(1.281, 1.360)	Unstable	Monotone
Fished & Stochastic	0	$1.51 + 0i$	1.51	(1.448, 1.568)	Unstable	Monotone
Control	248	$0.470 - 0.423i$	0.633	(0.440, 0.727)	Stable	Oscillatory
Fished	146	$0.634 + 0.626i$	0.890	(0.840, 0.972)	Stable	Oscillatory
Stochastic	236	$0.462 - 0.426i$	0.625	(0.430, 0.720)	Stable	Oscillatory
Fished & Stochastic	153	$0.677 + 0.611i$	0.912	(0.856, 0.954)	Stable	Oscillatory

589
590

591

Table A5. Characteristic return time around the non-zero equilibrium from equation (2). Return time is calculated as $T_R = 1/(1 - |\lambda|)$ with $F = 0$ to emphasize the intrinsic dynamics. Confidence intervals were bootstrapped using 10,000 random draws from a multivariate normal parameter distribution with means and variance-covariance matrix from the fitted model.

Treatment	N^*	$\lvert\lambda_{N^*}\rvert$	95% $CI_{\lvert\lambda\rvert}$	T_R	95% CI_{TR}
Control	248	0.633	(0.440, 0.727)	2.725	(1.786, 3.663)
Fished	146	0.890	(0.840, 0.972)	9.091	(6.250, 35.714)
Stochastic	236	0.625	(0.430, 0.720)	2.667	(1.754, 3.571)
Fished & Stochastic	153	0.912	(0.856, 0.954)	11.364	(6.944, 21.739)

592
593
594

Appendix B: Figures

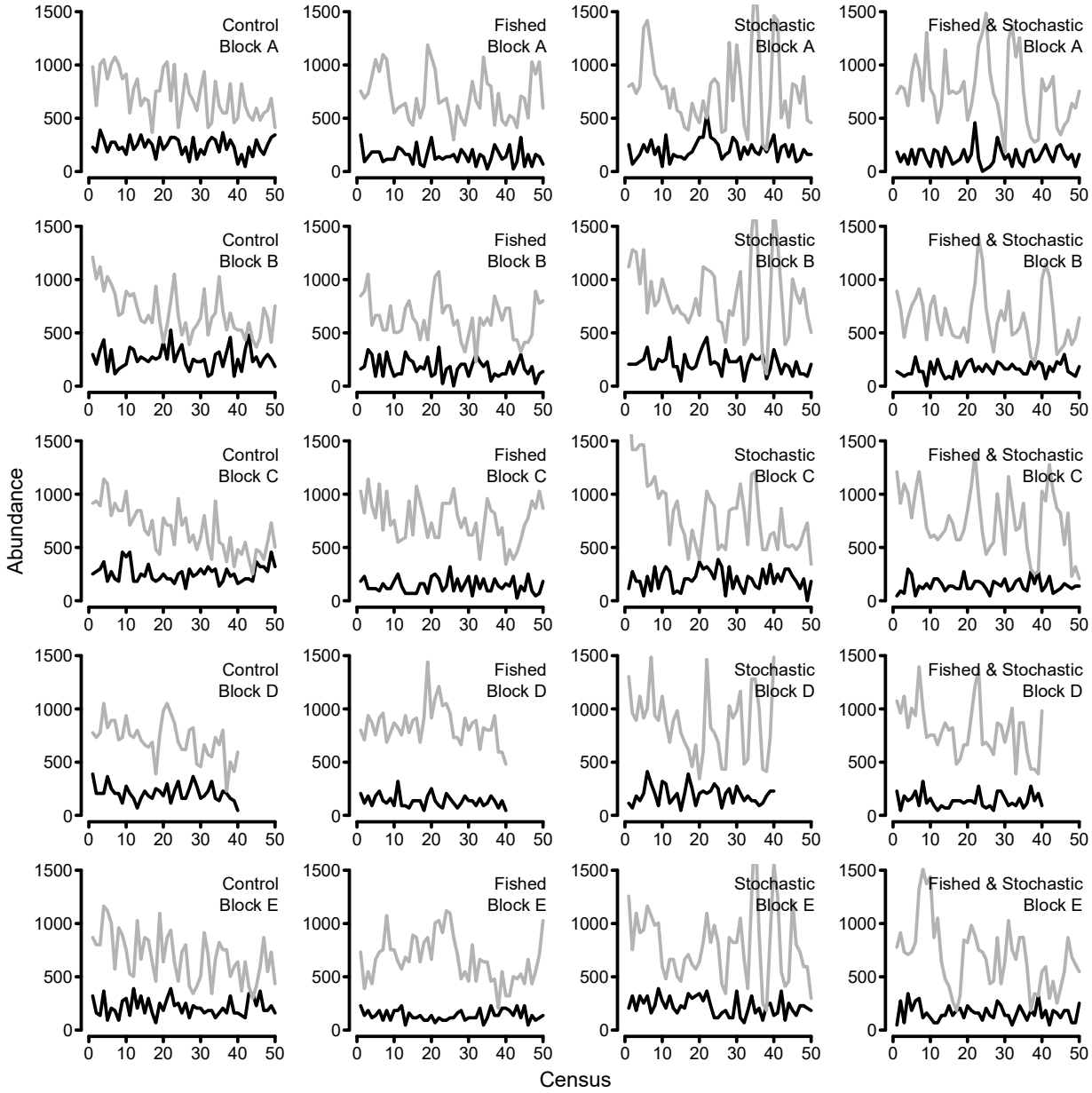

Figure B1. Abundance time series for juvenile (grey) and adult (black) *Daphnia*. Columns are: control, fished, stochastic, and fished & stochastic treatments, respectively. Rows are experimental blocks A–E.

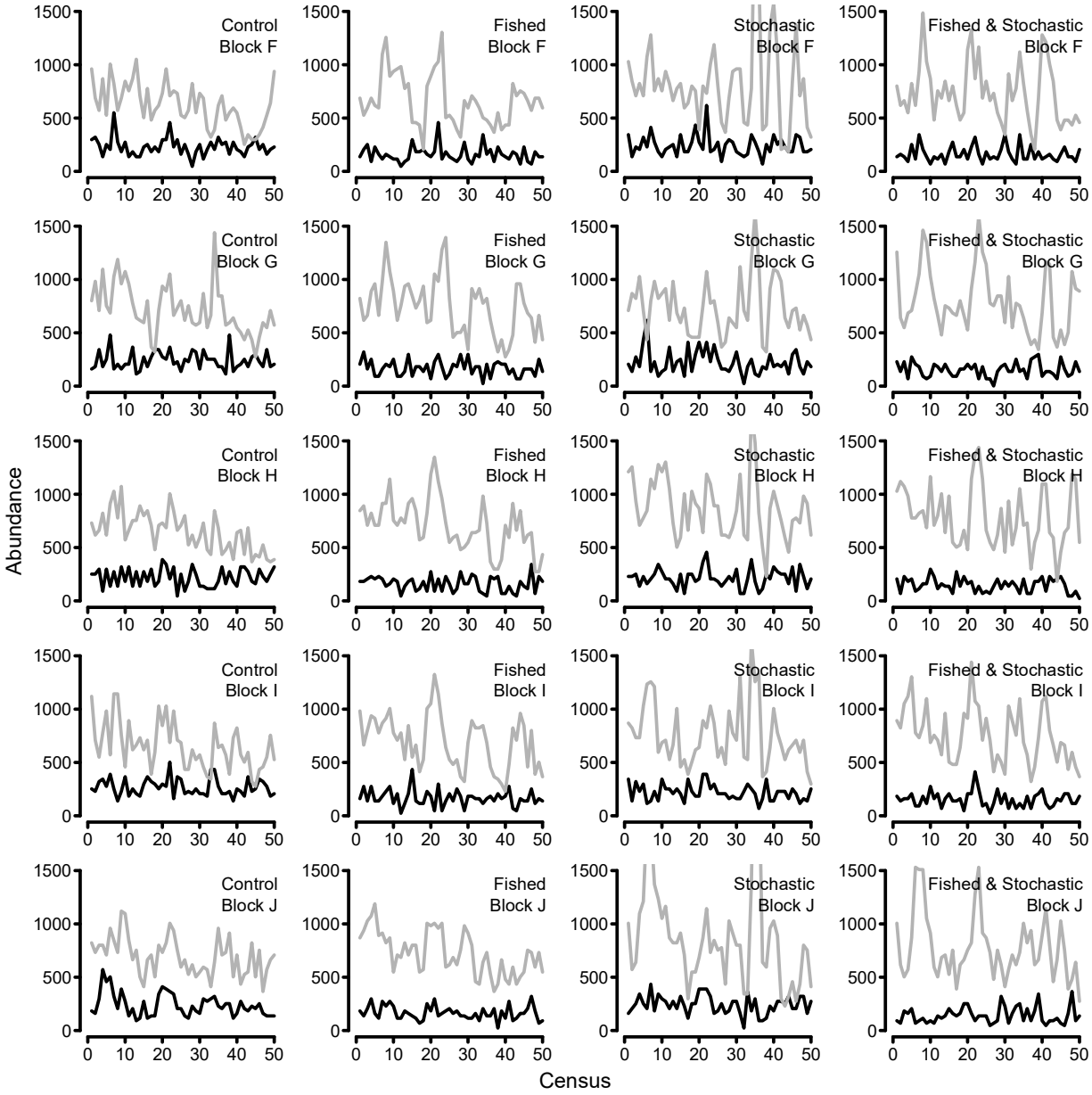

Figure B2. Abundance time series for juvenile (grey) and adult (black) *Daphnia*. Columns are: control, fished, stochastic, and fished & stochastic treatments, respectively. Rows are experimental blocks F–J.